Investigation of thermal energy atomic scattering from solid surfaces using the 3D time-dependent Schrödinger equation

G. Varga *

Technical University of Budapest, Physical Department, Budafoki s 8, Budapest 1111, Hungary

Abstract

The thermal energy atomic scattering from solid surfaces is very useful tool in the energy range of 10–100 meV because the usually applied He probe particles do not penetrate into the surface but provide information about the top layer. We focused on the scattering from ideally periodic and disordered surfaces. The physical model contains an appropriate 3D interaction potential and a 3D Gaussian wave-packet. The interaction potential describes the periodicity or the disorder of the surfaces. The Gaussian wave-packet characterises the atomic beam as an ensemble of independent particles with finite energy spread. The propagation of the Gaussian initial wave function has been determined by the solution of the 3D time-dependent Schrödinger equation. The probability density function has been rendered at the detector region in real space and in momentum space. The slices of the probability density function parallel to the surface provide the surface topography not only in the case of an ideally periodic surface structure but also in the case of disorder. © 1999 Elsevier Science B.V. All rights reserved.

1. Introduction

The thermal energy atomic scattering from solid surfaces (TEAS) is a useful surface tool to explore the solid surface top layer [1]. Diffractive scattering is a traditional TEAS measurement method. It is a well-discussed area of TEAS describing the entire process as a one particle and periodic interaction potential problem. The incoming wave is described by a plane wave and the surface is characterised by a periodic time-independent interaction potential. This method — using the Bragg conditions — answers the main question: 'What is the final intensity distribution of the diffraction peaks?'. The incoming particle beam, however, is not completely monoenergetic, and the disordered surface vibrates, too. The non-ideal elements cause attenuation of the diffractive peaks. A more realistic model has been chosen. The main components are the following:

- Gaussian wave-packet to describe the incoming particle beam;
- interaction potential without the restriction of periodicity and time independence.

The aim of the present paper is to investigate the scattering mechanism using the three-dimensional (3D) time-dependent Schrödinger equation (TDSE). This method gives a golden opportunity to trace the whole interaction process.

* Fax: +36-1-242-43-16.

E-mail address: vargag@phy.bme.hu (G. Varga)

2. The model

Quantum mechanics basically is able to account for the physical processes of TEAS. Under certain conditions, e.g. the probe particles are heavy atoms, a semiclassical model approach is appropriate [2,3]. This is the reason we work within the frame of quantum mechanics. The time-dependent Schrödinger equation has been applied, which corresponds to an initial value problem. This picture provides simple visualisation and physical interpretation. The physical space has been chosen large enough to contain the whole interaction region of TEAS. This means that at the starting point and at the end point of the time there is no interaction between the particle beam and the solid surface. The wave function stays in the chosen physical space. The incoming atomic beam is described by a plane wave in standard models. The plane wave is an interpretation of an absolutely monoenergetic atomic beam, which has no velocity and energy spread. However, as is known, supersonic atomic beams have a narrow FWHM, because the velocity of the atomic beam may reach few tenfold of local sound velocity. A Gaussian wave-packet provides an appropriate mean velocity and spread of velocity. The Gaussian wave-packet can be considered as a description of an ensemble of neutral atoms with minimised uncertainty in real and momentum space. What does the initial wave packet describe? It describes the collective behaviour of the particles of the atomic beam. The particles of an atomic beam do not interact with each other, but they have a special distribution of velocity and energy. The Gaussian wave-packet characterises the atomic beam as a special quantum ensemble of independent particles. A 3D Gaussian wave-packet has been chosen:

$$\Psi(x, y, z, t=0) = C \exp\left[-\frac{(x-x_0)^2}{2\sigma_1^2} - \frac{(y-y_0)^2}{2\sigma_2^2} - \frac{(z-z_0)^2}{2\sigma_3^2} \right] \exp(i\boldsymbol{k}\boldsymbol{r}), \quad (1)$$

where Ψ is the wave function, (x, y, z) are the Cartesian coordinates, t is the time, C is the normalisation constant, (x_0, y_0, z_0) is the average position at $t=0$, σ is the standard deviation, i is the complex unit, $\boldsymbol{k}$ is the wave number vector and $\boldsymbol{r}$ is the position vector.

Since we focus on model calculations of atomic beam scattering from an ideally periodic and disordered solid surface we employ simple time-independent interaction potentials. It should be emphasised that this model does not demand time independence (this case is published later). In the case of the first example (Section 4), a Lennard–Jones–Devonshire type of interaction potential has been chosen [4]:

$$V(x, y, z) = D \exp\{-2\alpha[z - \text{disorder}(x, y)]\}$$
$$\times \left\{ 1 - 2\beta\left[\cos\left(\frac{2\pi}{a} x\right) + \cos\left(\frac{2\pi}{a} y\right) \right] \right\}, \quad (2)$$

where D is the energy constant, α is the repulsive constant, β is the corrugation constant and a is the lattice constant, and $\text{disorder}(x, y)$ ensures the surface disorder.

A corrugated Morse interaction potential describes the Rh(311) surface (Section 5):

$$V(\boldsymbol{R}, z) = D(\exp\{-2\alpha[z - \zeta(\boldsymbol{R}) - \text{disorder}(x, y)]\}$$
$$- 2 \exp\{-\alpha[z - \zeta(\boldsymbol{R}) - \text{disorder}(x, y)]\}), \quad (3)$$

where $\zeta(\boldsymbol{R})$ is the corrugation function and $\boldsymbol{R}$ is parallel to the surface [5].

3. Numerical method

Let us consider the time-dependent Schrödinger equation:

$$i\hbar \frac{\partial \Psi(\boldsymbol{r}, t)}{\partial t} = H\Psi(\boldsymbol{r}, t),$$

where $\hbar$ is Planck's constant divided by 2π and H is the Hamiltonian. A propagation scheme and an operation of the Hamiltonian have to be applied. A splitting operator method has been chosen with a third-order accurate formula in time [6]. Splitting the Hamilton operator into two parts, for kinetic

energy operator A and potential energy operator B, we can write the exact formal solution: $\Psi(r, t+\Delta t)=\exp[-i\,\Delta t(A+B)/\hbar]\Psi(r, t)$, in the case of a time-independent potential. This solution is no longer exact for a time-dependent interaction potential, but ensures efficient time propagation in that case, too. Our computations have been executed in three-dimensional Cartesian coordinate space. The solution of the TDSE demands time propagation in every time step and requires a method to determine the effect of the Hamilton operator for the wave function. Fast Fourier transformation (FFT) has been applied to calculate $H\Psi$ at every time step, because FFT demands only $N \ln N$ and not $N \times N$ operations as required in the finite difference method (N is the number of the sample points). FFT is an exponentially convergent approximation and in momentum space the derivation means simple multiplication.

We have looked for the approximation to the $\exp[-i\Delta t(A+B)/\hbar]=\exp[\lambda(A+B)]$ operator with the help of the split formulae [7,8]. A general decomposition is the following non-symmetric splitting: $\exp(\gamma\lambda A/2) \exp(\gamma\lambda B) \exp[1/2(1-\gamma)\lambda A] \times \exp[(1-2\gamma)\lambda B] \exp[1/2(1-\gamma)\lambda A] \exp(\gamma\lambda B) \exp(\gamma\lambda A/2)$, where $\gamma=1/(2-2^{1/3})$. It has third-order accuracy in time [6]. Although this expression involves seven exponential operators, one can show by the computations that the numerical algorithms are more efficient than the algorithms based on the standard second-order accurate split operator formula.

To calculate $\exp(\gamma\lambda A/2)\Psi$ it is necessary to work in momentum space where $\exp(\gamma\lambda A/2)$ means a multiplication and a function evaluation. Then we have to go back to real space by an inverse FFT. The calculation of $\exp(\gamma\lambda B)$ means a multiplication and a function evaluation in real space.

It is relevant to control the reliability of the numerical procedure. We investigated an increasing interaction potential, which approached an infinite hard wall. The intensity distribution has been calculated and compared with the diffraction pattern from the hard corrugated wall model [9]. The test calculations underlined the correctness of the above-described procedure. In addition, we know the split operator method conserves the unitarity of the wave function if it does not reach the edge of the chosen region where the computations are executed [10]. It is worth determining the norm every time step to exclude the case mentioned above. The split operator method does not conserve the energy and the phase. This fact necessitates monitoring the average energy. Refining the grid in discrete Hilbert space, the average energy should show time independence when the Hamiltonian is time independent. The method of phase controlling is the reversal of the progress of time. One has to recover the original wave function with an appropriate accuracy. If there is a relevant difference — in both previous methods — the grid refining is inevitable. We found that when the average energy was accurate the phase error was negligible.

Not only can the time propagation be violated, but if the grid density is not high enough the top of the momentum region may be cut. Fortunately, this fact appears immediately in the average energy.

The numerical methods demand a corresponding scale of the parameters. This is why atomic units (a.u.) have been used in the computer programme.

4. Results and conclusions for He scattering on a model surface

A model He–solid surface system has been considered to investigate the physical processes of scattering in the quantum mechanical region. First of all a completely periodic solid surface was analysed in the case of an approximately 30 meV He beam. (Input data (a.u.) in Eq. (1): $x_0=y_0=18.13$, $z_0=16.67$, $\sigma_1=\sigma_2=\sigma_3=\sqrt{5}$, $k_x=k_y=0$, $k_z=-4$; input data (a.u.) in Eq. (2): $D=0.00012$, $\alpha=0.582$, $\beta=0.2$, $a=5.18$, disorder$(x, y)=0$.) As is known, the scattering process leads to a diffractive intensity distribution. A relevant question is what happens near the surface in the quantum region. To answer this problem parallel slices of the probability density function (PDF) of the scattered He atoms to the solid surface have been rendered as time propagated. The PDF can be obtained as the square of
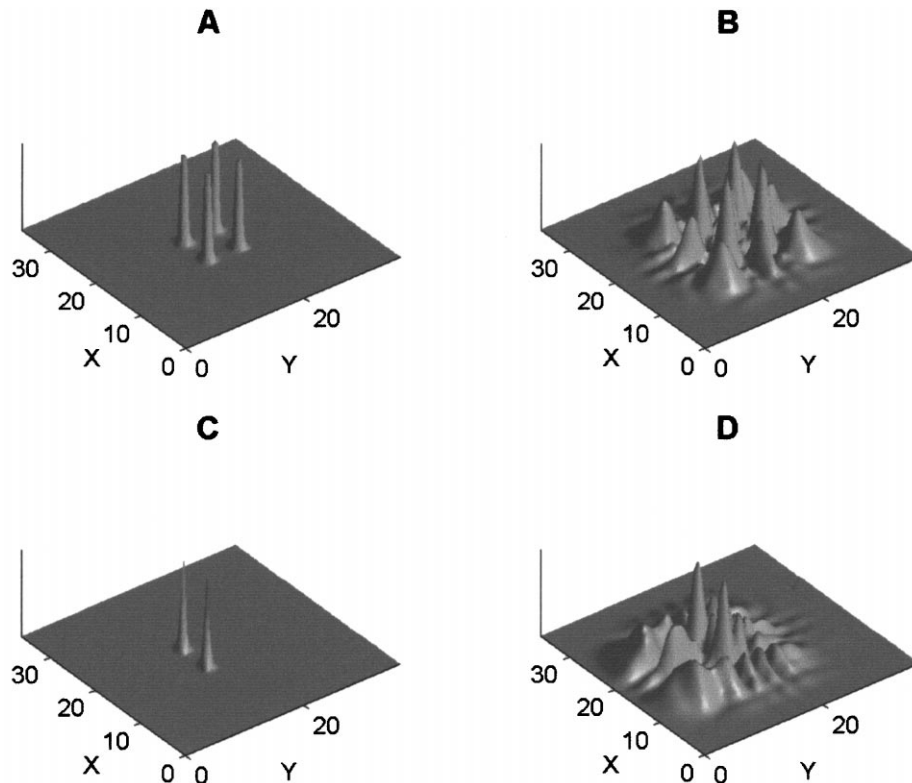
Fig. 1. Slices of the PDFs parallel to the surface in real space as time progresses in the case of periodic and stepped surface. (A) Wave-packet is in the quantum region of the interaction, near the periodic surface (around the classical turning point). (B) Wave-packet is far from the periodic surface after the interaction. (C) Wave-packet is in the quantum region of the interaction, near the stepped surface (around the classical turning point). (D) Wave-packet is far from the stepped surface after the interaction.

the absolute value of the wave function calculated by TDSE. In Figs. 1A and 2A one can see PDF in real and in momentum space, respectively. In momentum space the scattering channels can be discerned. The closed channels can be seen out of the Ewald circle. The intensity of the closed channels evanesces exponentially as time propagates, as the wave-packet moves from the surface. The open channels only provide the direction of the diffraction peaks if one considers energy conservation and the Bragg condition. The heights and width of the diffraction peaks continuously vary within the interaction region. Figs. 1B and 2B show the situation at the detector region, after scattering. The intensity distribution has shaped. One can see the Ewald circle directly near the surface in momentum space. However, the channels out of the Ewald region have disappeared

(closed channels). The diffraction peaks have more clear-cut contours than in real space. The shape of diffraction peaks mirrors the properties of a 3D realistic intensity distribution (e.g. the FWHM can be determined). Obviously, the diffraction peak intensities can be calculated quantitatively. Secondly, an irregularly stepped surface has been investigated [11]. The input data are the same as above, except that in Eq. (2) $disorder(x, y) = 2(\arctan\{2[y - \max(y)/2]\}/(\pi/2) + 1)/2$. The diffraction pattern has been deformed to the case of completely periodic surface. In Figs. 1C, 1D, 2C and 2D one can see an axis of symmetry of the diffraction pattern, which is parallel to the y direction. The position of the axis of symmetry of the diffraction pattern provides information on the direction of the step. The set of open channels has distorted to the case of an ideally periodic surface.

A
B

C
D
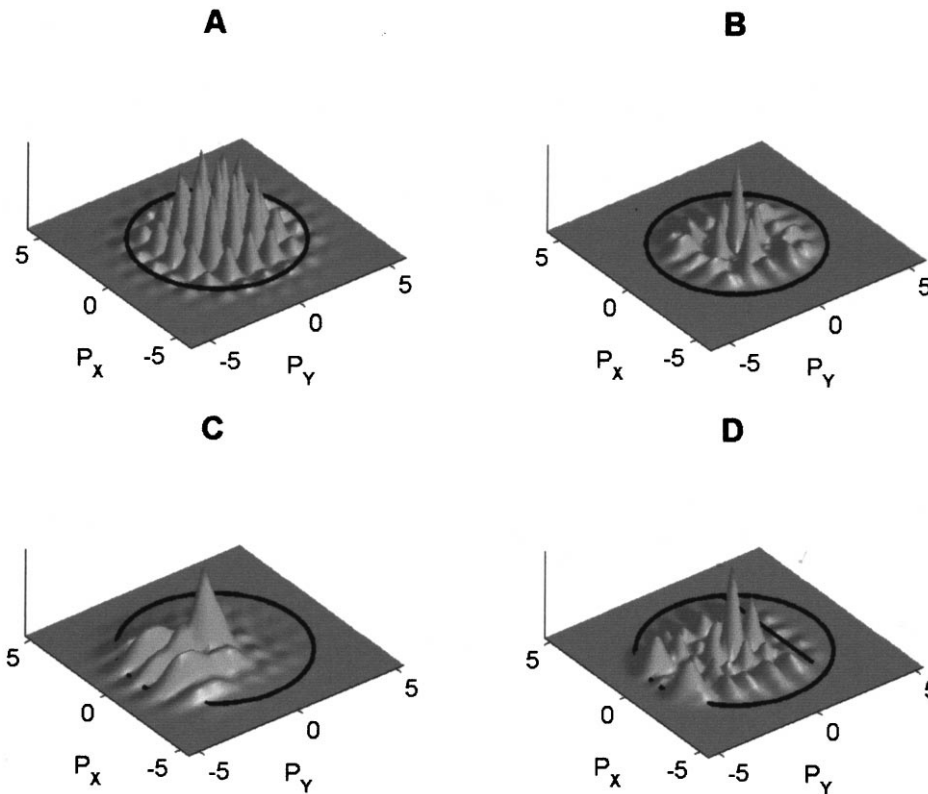
Fig. 2. Slices of the PDFs parallel to the surface in momentum space as time progresses in the cases of periodic and stepped surfaces. P_x and P_y are momenta in the x and y directions, respectively. Ewald circles have been drawn. (A) Wave-packet is in the quantum region of the interaction, near the periodic surface (around the classical turning point). (B) Wave-packet is far from the periodic surface after the interaction. (C) Wave-packet is in the quantum region of the interaction, near the stepped surface (around the classical turning point). (D) Wave-packet is far from the stepped surface after the interaction. The fault-line has been drawn as a black line.

On drawing the Ewald circle the diffraction directions move left. The 4 mm symmetry has disappeared, and only 1 m symmetry can be seen. A fault-line also appears because of the surface step. This line corresponds to the intensity minimum, which stems from the diffraction of two different planes of the stepped surface. In addition to this minimum line, a double-humped strong maximum has evolved. This is again the effect of the step, but now the appropriate waves amplify each other. One can see many smaller intensity peaks. These peaks have arisen from the electron density corrugation of the periodic regions. The full intensity distribution has arisen from the interference of the smoother electron density corrugation and the larger stepped surface. If the surface were com-pletely smooth the intensity pattern would not be so structured.

5. Results and conclusions for He scattering on the Rh(311) surface

Finally He scattering on the Rh(311) surface was simulated. An approximately 63 meV He beam was scattered on regularly (nominally) and irregularly (randomly) stepped Rh(311) surfaces [5,11]. The ordered Rh(311) surface is a regularly stepped surface. Input data (a.u.) in Eq. (1): $x_0 = 9.86$, $y_0 = 25.25$, $z_0 = 16.5$, $\sigma_1 = \sigma_2 = \sigma_3 = \sqrt{5}$, $k_x = k_y = 0$, $k_z = -5.831$. Input data in Eq. (3):
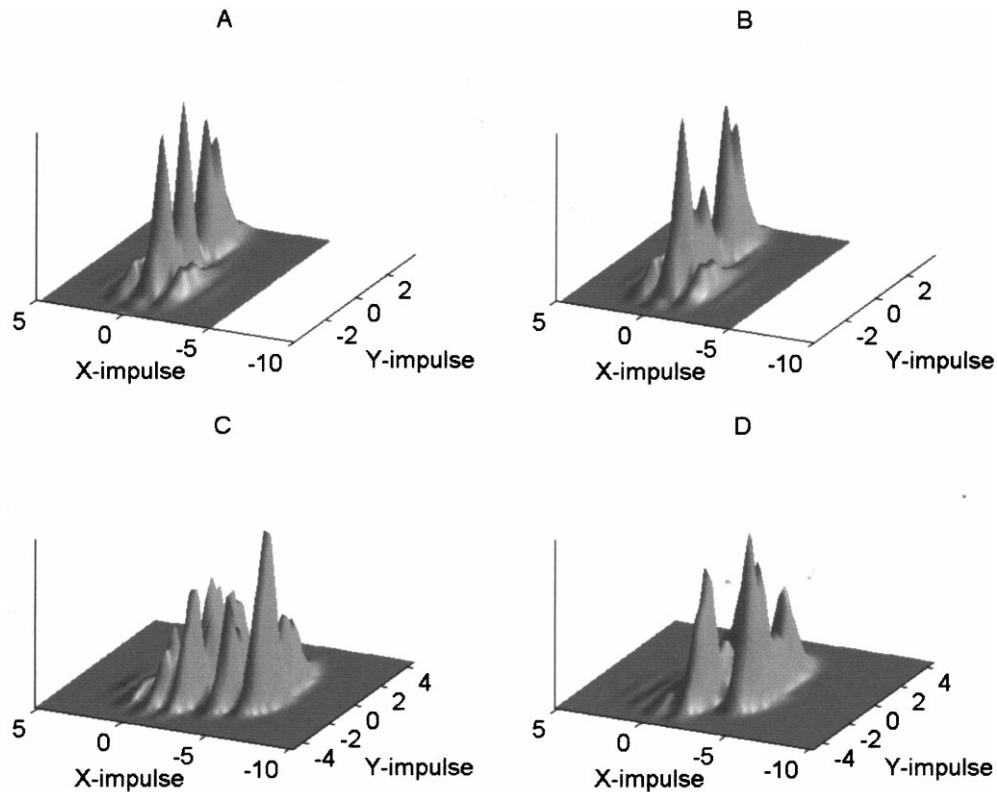
Fig. 3. He scattering on Rh(311). Slices of the PDFs parallel to the surface in momentum space as time progresses in the cases of regularly and irregularly stepped surfaces. P_x and P_y are momenta in the x and y directions, respectively. (A) Wave-packet is in the quantum region of the interaction, near the periodic surface (around the classical turning point). (B) Wave-packet is far from the periodic surface after the interaction. (C) Wave-packet is in the quantum region of the interaction, near the irregularly stepped surface (around the classical turning point). (D) Wave-packet is far from the irregularly stepped surface after the interaction.

$D = 7.74$ meV, $\alpha = 1.01$ Å^{-1}, disorder$(x, y) = 0$ and the parameters of the corrugation function have been chosen from the literature [5]. The corrugation parameters have been fitted to the experimental results by the hard corrugated wall model [5]. Obviously, Eq. (3) does not provide the effective corrugation function [12]. However, it is a good approach to the interaction potential in first order.

The top facet is partly lacking in the present example of the irregularly stepped Rh(311) surface. The step height is equivalent to the distance of the neighbouring facets (311):

$$h = \frac{2\pi}{|G(311)|} = \frac{a}{\sqrt{11}},$$

where G is the reciprocal lattice vector and $a =$

3.80 Å is the lattice constant of fcc Rh. The input data are the same as above, except that in Eq. (3) disorder$(x, y) = h(\arctan\{2[x - \max(x)/2]\}/(\pi/2) + 1)/2$. This step can be achieved using rough ion bombardment.

In the case of a regularly stepped Rh(311) surface Fig. 3A and B shows the scattering dynamic near the interaction region and the diffraction pattern at the detector region, respectively. The structure of the diffraction pattern in the interaction region is similar to the diffraction pattern in the detector region. A relevant property of this diffraction pattern is the dominance of the in plane scattering. There are only low order out-of-plane diffraction peaks with not too high intensities.

The irregularly stepped Rh(311) surface pro-

vides a significantly different diffraction pattern near the surface and in the detector region too (Fig. 3C and D). The step causes a richer intensity distribution near the surface, in the interaction region (Fig. 3C). Except for a few, the scattering channels do not decay in the detector region in the x direction (Fig. 3D). The other scattering channels evanesce. The out-of-plane diffraction becomes significant. Two well-separated domains of the intensity distribution appear. This effect stems from the diffraction on two different planes of the stepped surface as was discussed in Section 4.

The examples of this paper demonstrate that the present TDSE model is appropriate to analyse the dynamics of atom diffraction from solid surfaces. Simulations of different atom–solid surface systems give typical structures of the intensity distributions that describe the given atom–solid surface systems. Comparing the experimental results with the simulation results, the surface structure can be determined to first order. This advantage of the TDSE model may provide a useful theoretical tool in the thorough investigation of the atom–surface scattering.

References

[1] G. Comsa, Surf. Sci. 299–300 (1994) 77.

[2] B. Gumhalter, K Burke, D.C. Langreth, On the validity of the trajectory approximation in quasi-adiabatic atom–surface scattering, in: P. Varga, G. Betz (Eds.), 3S Symposium on Surface Science, Obertraun, Austria, 1991, p.35.

[3] G. Varga, in: S. Bohátka (Ed.), Proceedings 7th Vacuum Conference, Debrecen, Budapest, Hungary, Extended Abstracts (May 1997) , p. 234.

[4] A.T. Yinnon, R. Kosloff, Chem. Phys. Lett. 102 (1983) 216.

[5] R. Apel, D. Farías, H. Tröger, E. Kristen, K.H. Rieder, Surf. Sci. 364 (1996) 303.

[6] A.D. Bandrauk, H. Shen, Chem. Phys. Lett. 176 (1991) 428.

[7] M. Suzuki, J. Math. Phys. 32 (1991) 400.

[8] A. Rouhi, J. Wright, Comput. Phys. 9 (1995) 554.

[9] G. Varga, L. Füstöss, Surf. Sci. 243 (1991) 23.

[10] C. Leforestier, R.H. Bisseling, C. Cerjan, M.D. Feit, R. Friesner, A. Guldberg, A. Hammerich, G. Jolicard, W. Karrlein, H.-D. Meyer, N. Lipkin, O. Roncero, R. Kosloff, J. Comput. Phys. 94 (1991) 59.

[11] B. Poelsema, G. Comsa, Scattering of Thermal Energy Atoms from Disordered Surfaces, Springer, Berlin, 1989.

[12] D. Gorse, B. Salanon, F. Fabre, A. Kara, J. Perreau, G. Armand, J. Lapujoulade, Surf. Sci. 147 (1984) 611.